



Polímeros: Ciência e Tecnologia

E-ISSN: 1678-5169

abpol@abpol.org.br

Associação Brasileira de Polímeros
Brasil

Ramos Wellen, Renate Maria; Silveira Rabello, Marcelo; Araujo Júnior, Inaldo Cesar;
Macedo Fachine, Guilhermino José; Canedo, Eduardo Luis
Melting and crystallization of poly(3-hydroxybutyrate): effect of heating/cooling rates on
phase transformation

Polímeros: Ciência e Tecnologia, vol. 25, núm. 3, mayo-junio, 2015, pp. 296-304
Associação Brasileira de Polímeros
São Carlos, Brasil

Available in: <http://www.redalyc.org/articulo.oa?id=47042199009>

- How to cite
- Complete issue
- More information about this article
- Journal's homepage in redalyc.org

redalyc.org

Scientific Information System

Network of Scientific Journals from Latin America, the Caribbean, Spain and Portugal

Non-profit academic project, developed under the open access initiative

Melting and crystallization of poly(3-hydroxybutyrate): effect of heating/cooling rates on phase transformation

Renate Maria Ramos Wellen^{1*}, Marcelo Silveira Rabello², Inaldo Cesar Araujo Júnior³,
Guilhermino José Macedo Fechine⁴ and Eduardo Luis Canedo^{2,5}

¹*Departamento de Engenharia de Materiais, Universidade Federal de João Pessoa – UFPB, João Pessoa, PB, Brazil*

²*Departamento de Engenharia de Materiais, Universidade Federal de Campina Grande – UFCG, Campina Grande, PB, Brazil*

³*Departamento de Engenharia Química, Universidade Federal de Pernambuco – UFPE, Recife, PE, Brazil*

⁴*Centro de Pesquisa sobre Grafeno e Nano-Materiais – Mackgrappe, Universidade Presbiteriana Mackenzie, São Paulo, SP, Brazil*

⁵*Instituto de Tecnologia de Pernambuco – ITEP, Recife, PE, Brazil*

*wellen.renate@gmail.com

Abstract

We studied the crystallization and melting phenomena of poly (3- hydroxybutyrate) (PHB), a biodegradable and biocompatible semi-crystalline thermoplastic, obtained from renewable resources. Its high crystallinity motivated several studies on crystallization and melting behavior, and also on ways to increase the amorphous polymer fraction. The effect of heating and cooling rates on the crystallization and melting of commercial PHB was investigated by differential scanning calorimetry. Several rates, ranging from 2.5 to 20 °C min⁻¹, were used to study the phase changes during heating/cooling/reheating cycles. The results showed that PHB partially crystallizes from the melt during the cooling cycle and partially cold crystallizes on reheating, and that the relative amount of polymer crystallizing in each stage strongly depends on the cooling rate. The melt and cold crystallization temperatures, as well as the rates of phase change, depend strongly on the cooling and heating rates.

Keywords: PHB, DSC, crystallization, melting, kinetics.

1. Introduction

Consumer products based on polymers are produced in large quantities to fulfill the needs of modern society. Automotive, shipbuilding, textiles, electronic devices, food packing, healthcare, etc, are examples of industrial areas that use polymeric resins derived from natural or synthetic sources on the manufacture of products with specific properties. Most applications use conventional commodity and engineering thermoplastics. However, polymers produced from natural resources and biodegradable plastics are gaining increasing interest, not only in biomedical applications but also in packing and consumer products^[1-3]. Among these types of polymers, Poly (3-hydroxybutyrate) (PHB) is a very promising material, a semi-crystalline thermoplastic polymer that is biodegradable and biocompatible, and is obtained from renewable resources (mainly sugar cane) by biotechnological processes of low environmental impact^[4-7].

Ongoing research, intended on establishing PHB's properties and optimize its processing conditions, are reported in the literature with an expectation of extending the range of its application. One of the major problems with PHB is its high crystallinity that allied with a relatively high glass transition temperature, results in a very fragile material. This fact is an important limitation to the practical use of PHB. Material properties of semi-crystalline polymers are controlled by molecular and supra-molecular structures that

are frequently determined by the crystallization mechanisms. Consequently, the study of crystallization and melting behavior is critical to understand and control material properties and the processing required to obtain them^[8-15].

An experimental program was developed in order to understand the effect of thermal cycles on the phase transitions of the polymer. In this work the crystallization and melting phenomena in PHB was investigated by differential scanning calorimeter (DSC), applying thermal cycles of heating/cooling/reheating at rates ranging from 2.5 °C/min to 20 °C/min. DSC tests revealed that PHB may be crystallized from molten state, phenomenon known as melt crystallization, as well from the rubbery amorphous solid state, phenomenon known as cold crystallization. The characteristic phase change temperatures and temperature intervals, the rate of phase change, and the amount of each phase involved in the change were determined in terms of the cooling and heating rates.

2. Experimental

2.1 Materials

The poly(3-hydroxybutyrate) (PHB) polymer, actually a random copolymer with approximately 4% 3- hydroxyvalerate units, was supplied by PHB Industrial SA (Brazil). Thermal

transition temperatures of PHB are presented in Table 1. Melt crystallization (T_c) and melting peak (T_{MP}) temperatures were estimated during cooling and reheating, respectively, according to ASTM D-3418; values reported were obtained at cooling/heating rate of 10°C/min.

The molecular mass distribution was obtained with a Viscotek HT-GPC Module 350A GPC at 40°C, with a refractive index detector. The material was dissolved in chloroform and the filtered solution was injected into the equipment. Solvent flow rate was 1 mL/min and the columns were calibrated with narrow molecular weight polystyrenes. The molecular mass distribution curve of PHB is shown in Figure 1. From these data the number-average molar mass $M_N = 52$ kg/mol and the polydispersity index $M_w/M_N = 2.66$ were estimated.

2.2 Methods

2.2.1 Differential scanning calorimetry (DSC) measurements

Thermal analysis was performed in a Shimadzu DSC-60 differential scanning calorimeter, under a nitrogen flow of 50 mL/min to minimize oxidative degradation to which the PHB is prone^[8,16]. Samples of approximately 5 mg were wrapped with aluminum foil to minimize the effect of the polymer thermal conductivity, which may cause differential broadening and shifting of peak positions^[17]. A new specimen was used for each run. A blank curve was obtained for each heating/cooling/reheating stage to ensure that no contamination of the instrument had taken place. A thermal cycle in four stages was used: (1) heating from room temperature (approximately 30°C) to 195°C (first heating stage); (2) at this temperature the samples were held a constant temperature for 3 min to eliminate any residual crystallinity and erase previous thermal history; (3) after which the melt was cooled to -10°C (cooling stage), and then (4) reheated to 195°C (second heating or reheating stage). Tests were run at constant rates of heating and cooling of 2.5, 5, 7.5, 10, 15, and 20°C/min. Figure 2 shows typical DSC output with the indicated cycles. Four thermal events were identified in most DSC tests, namely, melting during the first heating stage (F_1), melt crystallization during cooling (C_1), cold crystallization during reheating (C_2), and, finally, a second melting event (F_2).

For each thermal event, the starting and end points of departure from the underlying baseline were visually established in a plot of energy flow (J) versus time (t). The fractional crystallization (or melting) x for the event was computed as a function of time by integration:

$$x(t) = \frac{1}{E_0} \int_{t_1}^t |J(t') - J_0(t')| dt' \quad (1)$$

where t_1 and t_2 were the initial and final times, J_0 is the virtual baseline during the event (straight in the present case), and E_0 is the total latent heat of phase change:

$$E_0 = \int_{t_1}^{t_2} |J(t) - J_0(t)| dt \quad (2)$$

Table 1. Thermal transition temperatures of PHB.

Polymer	T_g (°C)	T_c (°C)	T_{MP} (°C)
PHB	2	56.5	169

The rate of phase change (crystallization or melting) c is simply:

$$c(t) \equiv \frac{dx}{dt} = \frac{|J(t) - J_0(t)|}{E_0} \quad (3)$$

from which the peak (maximum) and average crystallization rates may be computed. The fractional crystallization/melting x and the rate of crystallization/fusion c may be expressed as functions of temperature (T), knowing the linear relationship between time and temperature during the event:

$$T = T_1 + \phi(t - t_1) \quad (4)$$

where T_1 is the sample temperature at the starting point t_1 , and ϕ is the (constant) rate of heating or cooling during the event. The specific latent heat of crystallization or melting (or enthalpy, since the phase change occurs at constant pressure) is computed from E_0 , polymer fraction w_p , and the sample mass m_s :

$$\Delta H = \frac{E_0}{w_p m_s} \quad (5)$$

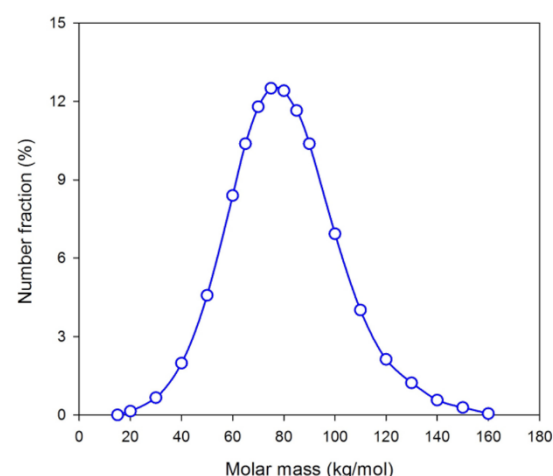


Figure 1. Molecular weight distribution curve of PHB used in this work.

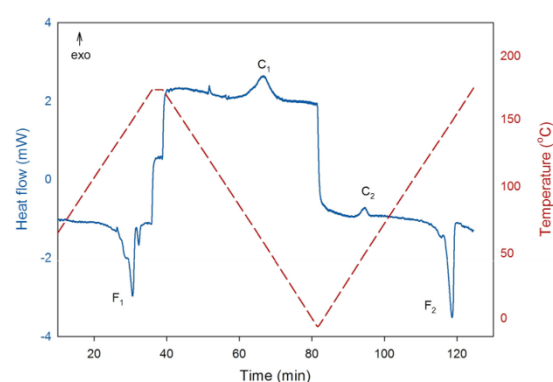


Figure 2. Typical DSC output for PHB heating/cooling/reheating at 5°C/min (exothermic peaks up), showing the phase change events: first melting (F_1), melt crystallization (C_1), cold crystallization (C_2), and second melting (F_2).

The mass crystallinity change X during the event is estimated taking into account the heat of fusion of PHB 100% crystalline ΔH_m° :

$$\Delta X = \frac{\Delta H}{\Delta H_m^\circ} \quad (6)$$

The value $\Delta H_m^\circ = 146 \text{ J/g}$ at the equilibrium melting temperature $T_M^\circ = 185^\circ\text{C}$ was reported in the literature^[18].

2.2.2 Heating and cooling rates

In heat flow DSC instruments the nominal heating and cooling rates are, at best, approximations to the rates of change of the reference temperature. True heating and cooling rates were computed from the sample temperature output of the DSC as:

$$\phi(t_i) = \frac{|T_{i+1} - T_{i-1}|}{2\Delta t} \quad (7)$$

where ϕ is the rate at time t_i ; T_{i-1} , T_{i+1} are the temperatures at times $t_i - \Delta t$ and $t_i + \Delta t$, and $\Delta t = 1 \text{ s}$ is time interval between measurements. True heating/cooling rates computed for the temperature intervals of the second fusion (heating) and melt crystallization (cooling) and presented in Table 2, along with their 95% confidence intervals. The deviations (σ) correspond to the RMS average point-to-point variation.

Table 2. True heating/cooling rates (in $^\circ\text{C/min}$).

ϕ_{nom}	On Cooling		On Heating	
	ϕ	σ	ϕ	σ
2.5	2.43 ± 0.08	1.42	2.40 ± 0.15	2.01
5.0	4.88 ± 0.10	1.46	4.79 ± 0.17	2.05
7.5	7.29 ± 0.01	0.07	7.25 ± 0.03	0.25
10	9.79 ± 0.15	1.17	9.57 ± 0.19	1.84
15	14.52 ± 0.02	0.13	14.42 ± 0.24	2.19
20	19.39 ± 0.15	1.16	19.25 ± 0.38	2.32

Part of this variation may be attributed to ‘numerical noise’ introduced during the commutation of ϕ . Figure 3 shows typical plots. Average real heating and cooling rates were found to be 2 to 4% lower than the nominal values. Considering that typical uncertainties in DSC measurements are of the order of 5%, the discrepancies found between nominal and ‘true’ heating/cooling rates are not a serious problem^[19].

3. Results and Discussion

3.1 DSC measurements

The DSC scans for heating, cooling and reheating stages, obtained according to the experimental procedure described above, are shown in Figure 4. Figure 4a presents the endotherms corresponding to the first melting of PHB, which takes place as double melting peaks, and may be affected by the injection molding process to which specimens were submitted. Figure 4b shows a crystallization event during cooling from the melt, in the form of broad peaks, particularly at low cooling rates. In addition to the second melting endotherms, Figure 4c shows a previous cold crystallization event (the exothermic peak) at all but the slowest heating/cooling rate (2.5°C/min).

Thus, under experimental conditions tested the first melting occurs as double melting peaks (a major peak, followed of a minor peak at *higher* temperature) and the second fusion is visualized as a single complex peak (with a shoulder – hidden peak – at a *lower* temperature). The crystallization occurs partially during the cooling stage (from the melt) and partially during the reheating stage (as cold crystallization). The relative areas of melt and cold crystallization peaks (related to the amount crystallized) depend on the rate during the cooling stage. No cold crystallization was detected at rates below 5°C/min (see Table 3); it is probable that during cooling stage at $\phi < 5^\circ\text{C/min}$ the all crystallizable polymer effectively crystallized from the melt.

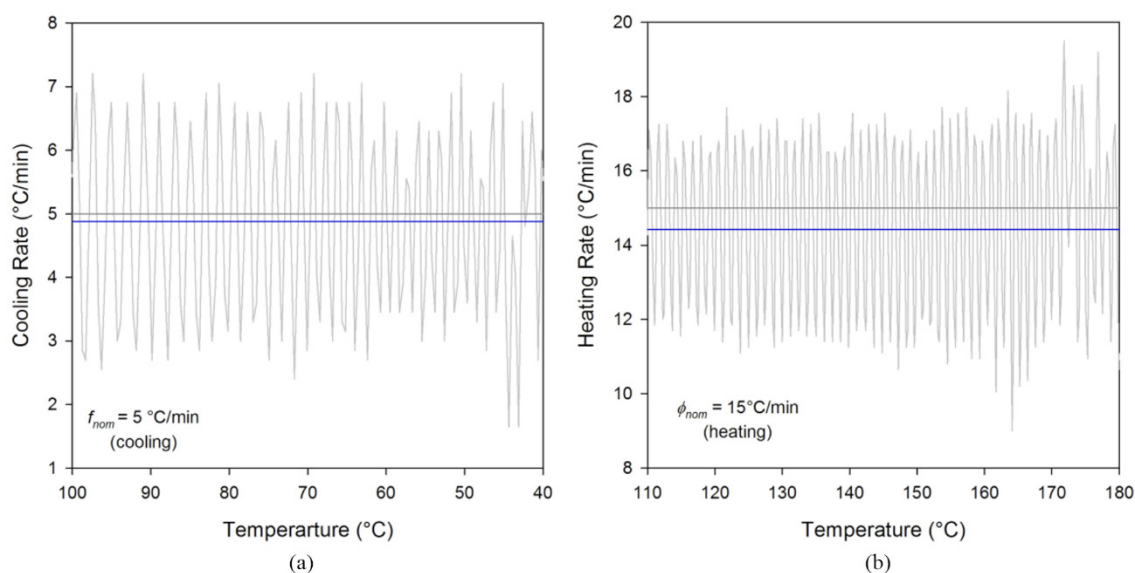


Figure 3. Typical real heating and cooling rates; cooling at nominal 5°C/min (a), heating at nominal 15°C/min (b). Horizontal black lines represent the average (real) heating/cooling rate in each case.

3.1.1 Crystallization analysis

Fractional crystallization versus time plots are presented in Figure 5 for the cooling/reheating rates tested, and some thermodynamic and kinetic parameters of both melt and cold crystallization are presented in Table 2.

The crystallization curves show the sigmoid shape characteristic of phase transformation processes in polymers. Macroscopic crystallization in polymers starts at very low rates due to the first, slow nucleation step; crystallization rate increases during the main or bulk crystallization and then decreases as the material is depleted of crystallizable molecules

and due to spherulitic impingement^[20-22]. Most crystallization parameters are strongly dependent on the cooling/reheating rate, and the dependence is different for the melt and cold crystallization processes. The crystallization temperature increases with the heating rate for the cold crystallization, while the opposite trend is observed for crystallization from the molten state. Moreover, cold crystallization is significantly faster than melt crystallization (notice the different time scale in Figures 5b and 5c).

Results presented in Figure 5 and Table 3 evidence differences in phase transformation processes for cold

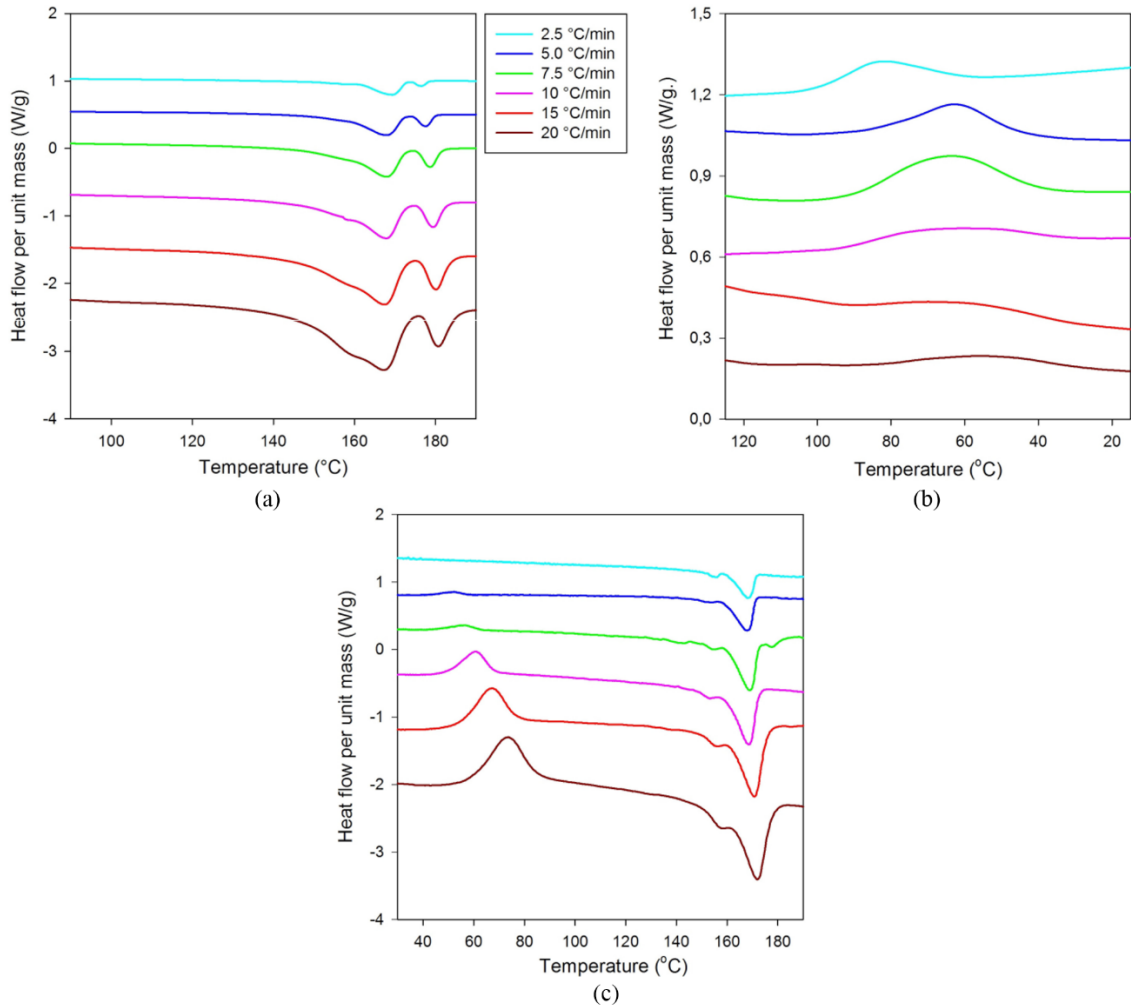


Figure 4. DSC scans obtained during the heating (a), cooling (b) and reheating (c) stages.

Table 3. Crystallization parameters determined during cooling and reheating stages.

ϕ_{NOM}	ϕ	Melt crystallization (C_1)						Cold crystallization (C_2)					
		T_c	ΔT_c	ΔH_c	c_{MAX}	$\tau_{1/2}$		T_c	ΔT_c	ΔH_c	c_{MAX}	$\tau_{1/2}$	
(°C/min)		(°C)	(°C)	(J/g)	(min ⁻¹)	(min)		(°C)	(°C)	(J/g)	(min ⁻¹)	(min)	
2.5	2.4	83.9	37.0	49.8	0.114	9.28	—	—	—	—	—	—	—
5	4.9	62.0	54.1	40.3	0.528	7.50	52.2	34.0	5.7	0.510	2.68		
7.5	7.3	64.5	53.6	39.9	0.228	4.70	55.8	19.6	6.7	0.642	1.95		
10	9.7	56.6	31.8	13.8	0.528	1.60	58.5	24.9	12.5	0.732	1.77		
15	14.5	60.0	51.7	5.4	0.414	2.20	67.1	30.9	32.8	0.990	1.67		
20	19.5	56.4	61.0	5.5	0.504	1.93	73.3	34.1	34.0	1.170	1.38		

crystallization (amorphous solid \rightarrow crystalline solid) and melt crystallization (fluid \rightarrow crystalline solid). Figure 6 shows graphically some of these trends.

Table 4 compares the crystallinity change determined during the cooling ΔX_c (C1) and reheating ΔX_c (C2) stages, as well as the total crystallinity change $\Delta X_c = \Delta X_c$ (C1) + ΔX_c (C2). The fraction of crystallizable polymer that crystallizes in each stage is a strong function of the cooling/heating rate. Figure 7 shows these results in graphical form.

The macroscopic trends revealed are consistent with moderately fast crystallization kinetics, overrun on cooling: it appears that at the faster cooling rates the material doesn't have enough time to complete crystallization before molecular motions slow down at low temperatures.

Considerations of the microstructure implication of these trends require a microkinetic study^[23-26] beyond the scope of this paper. However, the results presented in Tables 3, 4 and

Table 4. Crystallization parameters determined during cooling and reheating processes.

ϕ_{NOM}	ΔX_c (C ₁)	ΔX_c (C ₂)	ΔX_c	ΔX_c (C ₂)/ ΔX_c
(°C/min) (%)				
2.5	33.5	<0.5	33.5	0
5.0	27.6	3.9	31.5	0.124
7.5	27.3	4.6	31.9	0.144
10.0	9.5	8.6	18.0	0.475
15.0	3.7	22.5	26.2	0.859
20.0	3.8	23.3	27.1	0.861

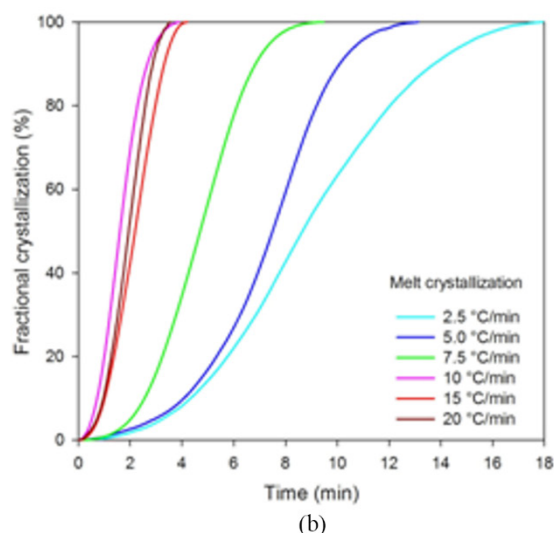
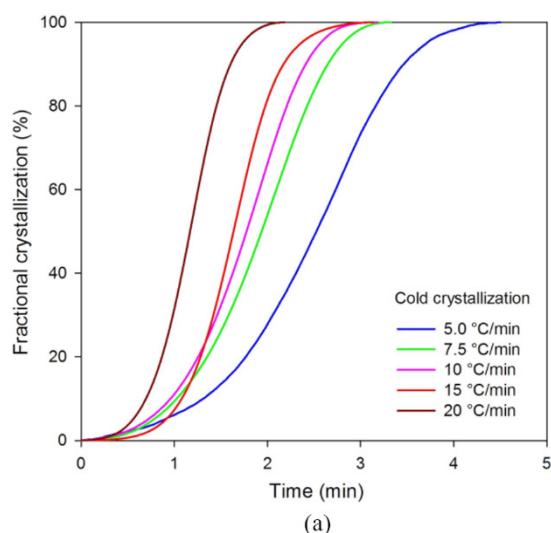


Figure 5. Fractional crystallization x (%) versus crystallization time t (min) for the melt crystallization (C₁) during the cooling stage (a) and for the cold crystallization (C₂) during the reheating stage (b).

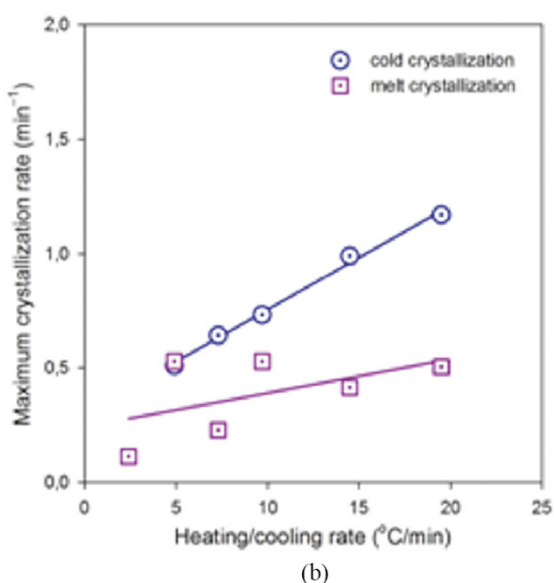
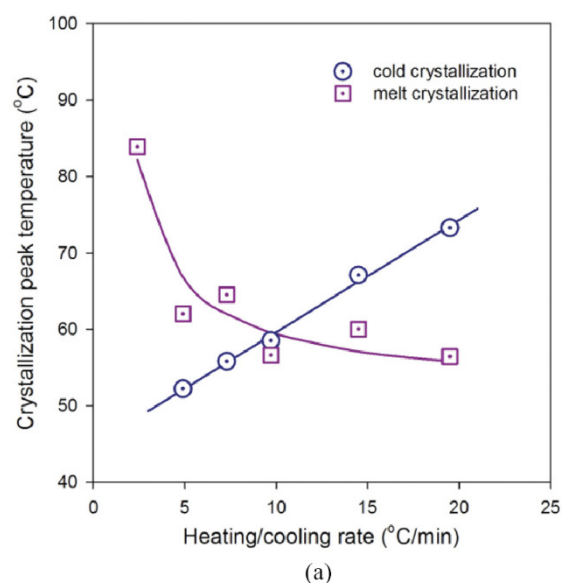


Figure 6. Crystallization temperature (a) and maximum crystallization rate (b) in terms of the cooling/heating rate, for the melt and cold crystallization processes.

Figures 6, 7 suggest that controlling the cooling/heating rate may result in crystals grown at different temperature intervals, perhaps with different stabilities and microstructures. From the literature it is known that the microstructure (the size and perfection of the crystalline entities), as well as the ratio of crystalline/amorphous phases, have direct influence on the properties of polymeric materials^[20,27-29].

3.1.2 Melting analysis

A complex peak structure was observed for the second melting event: a major peak preceded (and sometimes succeeded) by minor peaks that may be reduced to “shoulders” (hidden peaks) on the main peak. Multiple melting peaks may be attributed to the melting of different types of crystals, with different sizes and thermal stabilities. Specifically, small and less perfect crystals melt at lower temperature

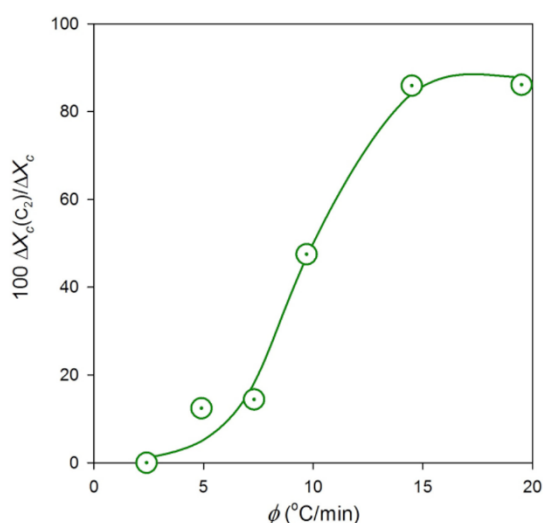


Figure 7. Fraction of crystallizable PHB that cold crystallizes, as a function of cooling/heating rate.

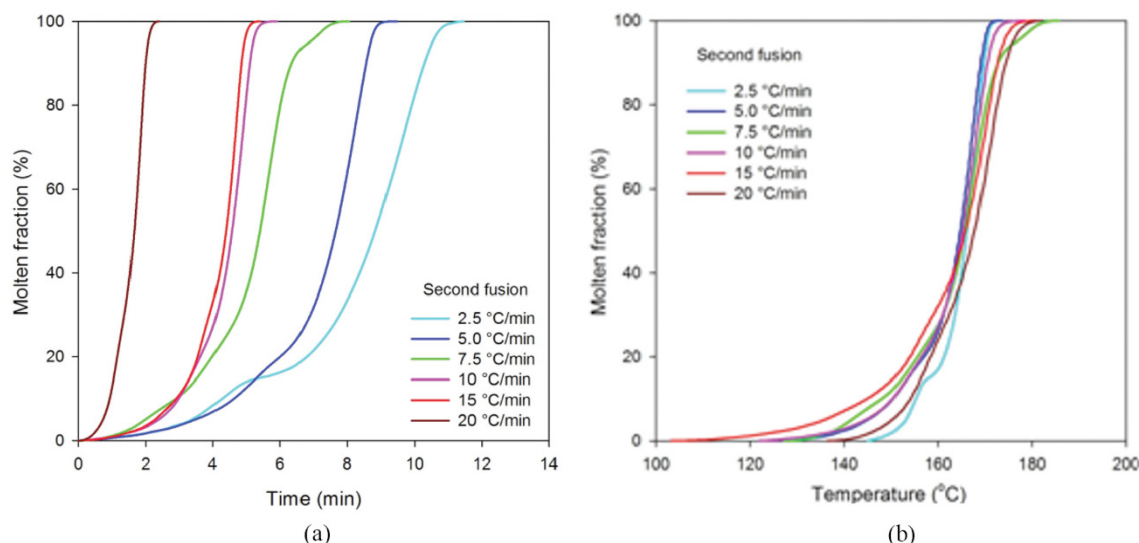


Figure 8. Evolution of molten fraction with time (a) and temperature (b) for the melting event during the reheating stage (F_2).

than the larger and more perfect ones. Multiple melting peaks observed by DSC are a rather common feature for many semi crystalline polymers, including polyesters. Multiple peaks may be attributed also to the existence of different crystal modifications, or to melting-recrystallization processes occurring during the DSC scan^[26,30-33].

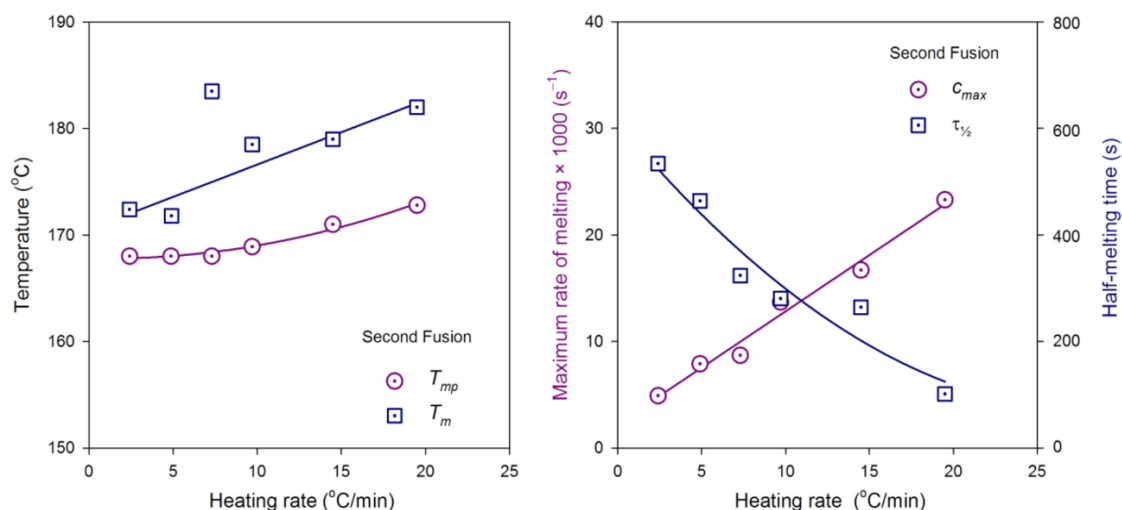
From DSC scans of Figure 4, the molten fraction x_F for the second fusion (F_2) during the reheating stage was computed by integration of the endothermic peaks. Figure 8 shows the plots of molten fraction as a function of time and temperature. Melting curves are also sigmoid; however, imperfect probably due to deformations caused the secondary peaks and shoulders observed in Figure 4c.

Table 5 presents some parameters determined during second melting event of the PHB, including the melting peak temperature T_{mp} and the temperature for 99% completion of melting T_m (which may be considered the true observed melting point of the resin, according to literature^[34] the temperature interval for the melting process ΔT_m , the latent heat of melting per unit mass ΔH_m , and the crystallinity (ΔX_c). Two measures of the kinetics of melting are included: the maximum melting rate c_{max} (the melting rate at the peak temperature) and the half-melting time $\tau_{1/2}$ (the time required to melt one-half of the polymer that melts, which is inversely proportional to average melting rate between $x_F = 0$ and $x_F = 0.5$).

A moderate increase of the melting temperature with the heating rate was observed, especially for the higher heating rates, and – consistently with the previous observations – a significant, almost linear, increase of the rate of fusion with increasing heating rate. Figure 9 shows these results in graphical form. The data in Tables 4 and 5 show that the total amount of crystallinity developed during the cooling/reheating cycles decreases at high cooling/heating rates ($\phi_{nom} > 7.5^\circ\text{C/min}$).

Table 5. Melting parameters determined during reheating process.

ϕ_{NOM} (°C/)	ϕ	T_{MP} (°C)	T_M	ΔT_M	ΔH_M (J/g)	X_C (%)	c_{MAX} (min ⁻¹)	$\tau_{1/2}$ (min)
2.5	2.4	168	172.4	23.0	59.9	41.0	0.294	8.90
5	4.9	168	171.8	36.4	66.6	45.6	0.474	7.73
7.5	7.3	168	183.5	47.4	88.0	60.3	0.522	5.40
10	9.7	169	178.5	42.1	57.2	39.2	0.822	4.68
15	14.5	171	179.0	58.8	62.4	42.7	1.002	4.40
20	19.5	173	182.0	35.5	50.5	34.6	1.398	1.70

**Figure 9.** Some measures of the thermodynamics and kinetics of melting determined during the reheating stage.

4. Conclusions

This paper presents a methodological procedure to study nonisothermal crystallization and melting phenomena in PHB by differential scanning calorimetry. The crystallization and melting behavior of PHB is strongly affected by the rates of cooling and heating. Increasing the cooling rate decreases the melt crystallization temperature and the amount of polymer that crystallizes from the molten state, and increases the rate of crystallization and the amount of polymer that cold crystallizes upon reheating. Increasing the reheating rate increases the cold crystallization temperature and the rate of crystallization from the amorphous solid phase, the total crystallinity developed is also affected, decreasing at high rates of cooling/heating within the interval studied. These findings suggest that the crystallinity of PHB may be controlled by the thermal cycles of heating and cooling to which the material is subjected.

5. Acknowledgements

The authors wish to thank PHB Industrial SA (Brazil) for supplying the PHB resin and Prof. Agnelli (UFSCar/Brazil) for molding the test specimens. The authors are also grateful to the *Conselho Nacional de Desenvolvimento Científico e Tecnológico* (CNPq/Brazil) and *Fundação de Amparo à Ciência e Tecnologia do Estado de Pernambuco* (FACEPE) for financial support.

6. References

- Bastioli, C. (2005). *Handbook of biodegradable polymers*. Shawbury: Rapra Technology.
- Zini, E., & Scandola, M. (2011). Green composites: an overview. *Polymer Composites*, 32(12), 1905-1915. <http://dx.doi.org/10.1002/pc.21224>.
- Reddy, M. M., Vivekanandhan, S., Misra, M., Bhatia, S. K., & Mohanty, A. K. (2013). Biobased plastics and bionanocomposites: current status and future opportunities. *Progress in Polymer Science*, 38(10-11), 1653-1689. <http://dx.doi.org/10.1016/j.progpolymsci.2013.05.006>.
- Doi, Y. (1990). *Microbial polyesters*. New York: Wiley-VCH.
- Hocking, P. J., & Marchessault, R. H. (1994). *Biopolymers (PHA)*. In G. J. L. Griffin (Ed.), *Chemistry and technology of biodegradable polymers* (pp. 1-154). London: Chapman & Hall/Backie.
- Hodzic, A. (2005). *Bacterial polyester-based biocomposites: a review*. In A. K. Mohanty, M. Misra & L. T. Drzal (Eds.), *Natural fibers, biopolymers, and biocomposites* (pp. 597-616). Boca Raton: Taylor & Francis/CRC Press.
- Philip, S., Keshavarz, T., & Roy, I. (2007). Polyhydroxyalkanoates: biodegradable polymers with a range of applications. *Journal of Chemical Technology and Biotechnology*, 82(3), 233-247. <http://dx.doi.org/10.1002/jctb.1667>.
- Gogolewski, S., Jovanovic, M., Perren, S. M., Dillon, J. G., & Hughes, M. K. (1993). The effect of melt-processing on the degradation of selected polyhydroxyacids: polylactides, polyhydroxybutyrate, and polyhydroxybutyrate-co-valerates. *Polymer Degradation & Stability*, 40(3), 313-322. [http://dx.doi.org/10.1016/0141-3910\(93\)90137-8](http://dx.doi.org/10.1016/0141-3910(93)90137-8).

9. Gunaratne, L. M. W. K., & Shanks, R. A. (2005). Multiple melting behaviour of poly(3-hydroxybutyrate-co-hydroxyvalerate) using step-scan DSC. *European Polymer Journal*, 41(12), 2980-2988. <http://dx.doi.org/10.1016/j.eurpolymj.2005.06.015>.
10. Reddy, C. S., Ghai, R., Rashmi, & Kalia, V. C. (2003). Polyhydroxyalkanoates: an overview. *Bioresource Technology*, 87(2), 137-146. [http://dx.doi.org/10.1016/S0960-8524\(02\)00212-2](http://dx.doi.org/10.1016/S0960-8524(02)00212-2). PMID:12765352.
11. Renstad, R., Karlsson, S., Albertsson, A. C., Werner, P. E., & Westdahl, M. (1997). Influence of processing parameters on the mass crystallinity of poly(3-hydroxybutyrate-co-3-hydroxyvalerate). *Polymer International*, 43(3), 201-209. [http://dx.doi.org/10.1002/\(SICI\)1097-0126\(199707\)43:3<201::AID-PI761>3.0.CO;2-7](http://dx.doi.org/10.1002/(SICI)1097-0126(199707)43:3<201::AID-PI761>3.0.CO;2-7).
12. Yoshie, N., Fujiwara, M., Ohmori, M., & Inoue, Y. (2001). Temperature dependence of cocrystallization and phase segregation in blends of poly(3-hydroxybutyrate) and poly(3-hydroxybutyrate-co-3-hydroxyvalerate). *Polymer*, 42(21), 8557-8563. [http://dx.doi.org/10.1016/S0032-3861\(01\)00408-6](http://dx.doi.org/10.1016/S0032-3861(01)00408-6).
13. Ziaee, Z., & Supaphol, P. (2006). Non-isothermal melt- and cold-crystallization kinetics of poly(3-hydroxybutyrate). *Polymer Testing*, 25(6), 807-818. <http://dx.doi.org/10.1016/j.polymertesting.2006.04.009>.
14. Abdelwahab, M. A., Flynn, A., Chiou, B., Imam, S., Orts, W., & Chiellini, E. (2012). Thermal, mechanical and morphological characterization of plasticized PLA-PHB blends. *Polymer Degradation & Stability*, 97(9), 1822-1828. <http://dx.doi.org/10.1016/j.polymdegradstab.2012.05.036>.
15. Canetti, M., Urso, M., & Sadocco, P. (1999). Influence of the morphology and of the supermolecular structure on the enzymatic degradation of bacterial poly(3-hydroxybutyrate). *Polymer*, 40(10), 2587-2594. [http://dx.doi.org/10.1016/S0032-3861\(98\)00503-5](http://dx.doi.org/10.1016/S0032-3861(98)00503-5).
16. El-Hadi, A., Schnabel, R., Straube, E., Müller, G., & Riemschneider, M. (2002). Effect of melt processing on crystallization behavior and rheology of poly(3-hydroxybutyrate) (PHB) and its blends. *Macromolecular Materials and Engineering*, 287(5), 363-372. [http://dx.doi.org/10.1002/1439-2054\(20020501\)287:5<363::AID-MAME363>3.0.CO;2-D](http://dx.doi.org/10.1002/1439-2054(20020501)287:5<363::AID-MAME363>3.0.CO;2-D).
17. Wagner, M. (2010). *Thermal analysis in practice*. Schwerzenbach: Mettler-Toledo.
18. Barham, P. J., Keller, A., Otun, E. L., & Holmes, P. A. (1984). Crystallization and morphology of a bacterial thermoplastic: poly-3-hydroxybutyrate. *Journal of Materials Science*, 19(9), 2781-2794. <http://dx.doi.org/10.1007/BF01026954>.
19. Höhne, G. W. H., Hemminger, W. F., & Flammersheim, H. J. (2010). *Differential scanning calorimetry* (2nd ed.). Berlin: Springer.
20. Wellen, R. M. R., & Rabello, M. S. (2005). The kinetics of isothermal crystallization and tensile properties of poly(ethylene) terephthalate. *Journal of Materials Science*, 40(23), 6099-6104. <http://dx.doi.org/10.1007/s10853-005-3173-3>.
21. Ziaee, Z., & Supaphol, P. (2006). Non-isothermal melt- and cold-crystallization kinetics of poly(3-hydroxybutyrate). *Polymer Testing*, 25(6), 807-818. <http://dx.doi.org/10.1016/j.polymertesting.2006.04.009>.
22. Wellen, R. M. R., & Rabello, M. S. (2009). Antinucleating action of polystyrene on the isothermal cold crystallization of poly(ethylene terephthalate). *Journal of Applied Polymer Science*, 114(3), 1884-1895. <http://dx.doi.org/10.1002/app.29569>.
23. Shafee, E. E., & Ueda, W. (2002). Crystallization and melting behavior of poly(ethylene oxide)/poly(*n*-butyl methacrylate) blends. *European Polymer Journal*, 38(7), 1327-1335. [http://dx.doi.org/10.1016/S0014-3057\(02\)00018-6](http://dx.doi.org/10.1016/S0014-3057(02)00018-6).
24. An, Y., Dong, L., Mo, Z., Liu, T., & Feng, Z. (1998). Nonisothermal crystallization kinetics of poly(β -hydroxybutyrate). *Journal of Polymer Science: Part B, Polymer Physics*, 36(8), 1305-1312. [http://dx.doi.org/10.1002/\(SICI\)1099-0488\(199806\)36:8<1305::AID-POLB5>3.0.CO;2-Q](http://dx.doi.org/10.1002/(SICI)1099-0488(199806)36:8<1305::AID-POLB5>3.0.CO;2-Q).
25. Wellen, R. M. R., & Rabello, M. S. (2007). Redução da velocidade de cristalização a frio do PET na presença de poliestireno. *Polímeros: Ciência e Tecnologia*, 17(2), 113-122. <http://dx.doi.org/10.1590/S0104-14282007000200010>.
26. Wellen, R. M. R., Canedo, E. L., & Rabello, M. S. (2011). Nonisothermal cold crystallization of poly(ethylene terephthalate). *Journal of Materials Research*, 26(9), 1107-1115. <http://dx.doi.org/10.1557/jmr.2011.44>.
27. Blundell, D. J., Liggat, J. J., & Flory, A. (1992). The crystal lamellar morphology of an aromatic polyketone with unusual crystallization and melting behavior. *Polymer*, 33(12), 2475-2482. [http://dx.doi.org/10.1016/0032-3861\(92\)91127-N](http://dx.doi.org/10.1016/0032-3861(92)91127-N).
28. Blundell, D. J., & Osborn, B. N. (1983). The morphology of poly(aryl-ether-ether-ketone). *Polymer*, 24(8), 953-958. [http://dx.doi.org/10.1016/0032-3861\(83\)90144-1](http://dx.doi.org/10.1016/0032-3861(83)90144-1).
29. Varma, P., Lofgren, E. A., & Jabarin, S. A. (1998). Properties and kinetics of thermally crystallized oriented poly(ethylene terephthalate) (PET). II. Physical and optical properties. *Polymer Engineering and Science*, 38(2), 245-253. <http://dx.doi.org/10.1002/pen.10185>.
30. Gunaratne, L. M. W. K., & Shanks, R. A. (2005). Melting and thermal history of poly(hydroxybutyrate-co-hydroxyvalerate) using step-scan DSC. *Thermochimica Acta*, 430(1-2), 183-190. <http://dx.doi.org/10.1016/j.tca.2005.01.060>.
31. Harding, K. G., Dennis, J. S., von Blottnitz, H., & Harrison, S. T. (2007). Environmental analysis of plastic production processes: comparing petroleum-based polypropylene and polyethylene with biologically-based poly-beta-hydroxybutyric acid using life cycle analysis. *Journal of Biotechnology*, 130(1), 57-66. <http://dx.doi.org/10.1016/j.jbiotec.2007.02.012>. PMID:17400318.
32. Papageorgiou, G. Z., & Karayannidis, G. (1999). Multiple melting behaviour of poly(ethylene-co-butylene naphthalate-2,6-dicarboxylate)s. *Polymer*, 40(19), 5325-5332. [http://dx.doi.org/10.1016/S0032-3861\(98\)00746-0](http://dx.doi.org/10.1016/S0032-3861(98)00746-0).
33. Renstad, R., Karlsson, S., Albertsson, A. C., Werner, P. E., & Westdahl, M. (1997). Influence of processing parameters on the mass crystallinity of poly(3-hydroxybutyrate-co-3-hydroxyvalerate). *Polymer International*, 43(3), 201-209. [http://dx.doi.org/10.1002/\(SICI\)1097-0126\(199707\)43:3<201::AID-PI761>3.0.CO;2-7](http://dx.doi.org/10.1002/(SICI)1097-0126(199707)43:3<201::AID-PI761>3.0.CO;2-7).
34. Menczel, J. D., & Prime, R. B. (2009). *Thermal analysis of polymers*. New York: Wiley.

Received: Oct. 11, 2014

Revised: Nov. 29, 2014

Accepted: Jan. 09, 2015

List of symbols

c_{max} Maximum crystallization/melting rate (at T_c or T_{mp})

$E0$ Total latent heat released or absorbed by the sample during the crystallization or melting event

J Heat flow; rate of thermal energy exchanged between sample and the surroundings

$J0$ Virtual base line during a phase change event

mS Mass of the sample

T_c Peak crystallization temperature

T_{mp} Peak melting temperature

T_m Melting point (temperature at 99% of the amount molten)

$\tau_{1/2}$ Crystallization/melting half-time (time to attain 50% fractional crystallization/melting), inversely proportional to the mean crystallization/melting rate between 0 and 50% fractional crystallization/fusion

x fractional crystallization during a crystallization event

x_F molten fraction during a melting event

ϕ_{nom} Nominal (set) heating/cooling rate

ϕ True mean heating/cooling rate (computed by Equation 7)

ΔT_c Crystallization interval (from 1% to 99% of the amount crystallized)

ΔT_m Melting interval (from 1% to 99% of the amount melted)

ΔH_c Specific latent heat of crystallization

ΔH_m Specific latent heat of melting

ΔX_c Mass crystallinity (total)

$\Delta X_c(C1)$ Crystallinity developed during the crystallization from the melt event (C1)

$\Delta X_c(C2)$ Crystallinity developed during the cold crystallization event (C2)